ENGINEERING RESEARCH JOURNAL (ERJ)

Vol. 1, No. 44 April 2020, pp.22-28.

Journal Homepage: erj.bu.edu.eg

Laser cladding of Aluminum powder and its composite with SiCp and Mo on mild steel substrate: clad layer formation and surface topography

Aly Elkoussy, Mohamed A. Taha, Ahmed M. Elsabagz and Ahmed Farid

1 Faculty of engineering, Ain-Sham University (ASU), Cairo - Egypt

Abstract

Coating steel surfaces with hard ceramic particles in Aluminum has a great influence to improve mechanical properties and wear resistance. This research investigated direct laser deposition, where no binder is used, of pure Aluminum and its composite powder with SiCp of 30% and Mo 30% are conducted, applying laser cladding technique (LC) using coaxial cladding nozzle. The effects of SiCp and Mo content in composite and the laser processing parameters namely; laser power of 900 to 1200 watt, scan speed of 0.9 to 1.1 m.min^{-1} on clad layer formation and its geometry are studied. Results indicate that the clad layer forms gradually with increasing laser energy density first as aligned globular weakly bonded stacks then aligned tracks gradually overlapping, and finally a complete strong-bonded clad layer all over the specimen area, with surface waviness. The minimum clad surface waviness is obtained at the maximum laser energy density applied of 25.6 J.mm^{-2}. Clad layer detachment phenomenon was also observed at high laser energy density.

Keyword: Laser Cladding, Silicon Carbide, Tungsten carbide.

1. Introduction

Laser cladding is widely applied process in different industries and services such as medical, aerospace, and automotive industries (1,2). It is well known for improving the surface properties via deposition of desired layer on a substrate (3), which provides a durable, corrosion-resistant, or wear resistant layer (4,5). Different powder types are used such as; metallic powders (2,6,7),ceramic powders (8) and mixture of metallic and ceramic powders (MMC) (9,10).

Aluminum characterized by light weight and strong corrosion resistance, so they are used in different industrial fields (11). On the other side its low hardness and wear resistance minimize its use in the field of pumps , valves and machines(12). A possible solution to enhance the wear resistance and hardness of Aluminum, by adding hard ceramic particles by laser cladding technique(13), such as SiC (14,15) , TiC(16), a mixture of Cr_3C_2 and Cr, or mixture of Ti and SiC (16).

Clad layer formation process by laser has been investigated only by few number of previous researchers. The effect of laser power on clad layer geometry was conducted in case of SiCp depositing on vacuum-sintered substrates of (X2CrNiMo 17-12-2) austenitic, (X6Cr13) ferritic and (X2CrNiMo 22-8-2) duplex stainless steels using high power diode laser between 0.7 and 2.1 KW, at constant scanning rates between 0.3 and 0.5 m/min(17). In this research, penetration depth and width of clad surface were noticed to increase as the laser power increases, where a good surface quality approach was obtained at high laser power of 1.2 KW and scan speed of 0.9 m.min^{-1}.

To determine the quality of clad surface, researchers investigated some parameters such as surface shape, geometry and defect. Smooth surface shape, acceptable geometry and free of defect are evidence of clad quality(19). To enhance the quality it was found that maximizing the deposition rate, minimizing dilution, and elimination of defects are needed. While implementing, it is hard to get a cladding layer that meets all quality aspects. The compromise of processing parameters is essential to achieve acceptable clad layer quality (20).

The objective of this study is to develop hard clad layer on mild steel substrate by depositing pure aluminum powder /Mo and pure aluminum powder /SiCp powder composite mixture. The work is a systematic experimental investigation on clad layer formation and surface topography, in direct laser deposition of the powder mixture. The influence of laser processing parameters on the progress of layer formation, pore and crack formation and deposited layer topography are studied. The aim is to determine the conditions at which a uniform clad layer is formed with least defects.

2. Experimental Work

The powder used for deposition is mixtures of gas atomized aluminum (Al: 45-90 µm), tungsten carbide powders (Mo: 45-90 µm) and (SiC: 45-90 µm), both with particle sizes less than 125 µm. The substrate is a mild steel 15 x100 mm surface dimensions and 10 mm thick.

The laser used in this research was at the CSIR-NLC in Pretoria, South Africa. It consist of a 4.4kW Nd; YAG laser system. It is focused using a series of mirrors that reflect the laser beam into the precise location that it is needed. The laser head is then positioned to a height that gives the laser beam a desired diameter for the particular sample. The laser was manipulated using an 8-axis Kuka robot arm that can be programmed to produce the desired part.

The applied scan speeds are 0.9, 1 and 1.1 $m.min^{-1}$ and the laser powers are 0.9, 1, 1.1, and 1.2 KW. The powder feed rate is 1.8 $g.min^{-1}$. Five overlapped tracks and double layer were produced at the different laser powers and scanning speeds applied.

Laser energy density (applied energy per unit area, **E, $J.mm^{-2}$**) is used in this work as to express the laser processing parameters (9), as calculated by the following equation (19):

$$E = (4P/\pi * d * v) \quad \text{Eq. 1}$$

Where P is the laser power (watt), d is the focus diameter (mm), ν is the scanning speed (mm/s).

The clad samples are cut by wire cut F1 EDM wire cutting machine and are polished by 320, 400, 600, 800, and 1000 sandpaper. No Etchant was used. Olympic metallurgical microscope type PME with magnification up to X500, equipped with Panasonic digital camera.

3 Results and discussions

3.1 Powder catchment efficiency

To achieve best clad layer we have to maximize the powder deposition. Experimently it is hard to control the laser cladding process due to massive interference between injecting powders, substrate and laser beam (21).Powder deposition is evaluated through powder catchment efficiency, η, which is the ratio of the deposited powder in the cladding track to the total injected powder, which depends on different parameters such as; laser beam properties, nozzle standoff, powder particle size, powder jet velocity, cladding nozzle geometry and injection conditions. Moreover, the adhesion mechanism between the powder particles and the substrate influence the deposition rate of powder (19).

In these experiments, catchment efficiency has been evaluated using weight method that depends on the difference in weight of sample before and after deposition by equation of (19–21);

$$\eta = 100 * (w_a - w_b) / w_i \quad \text{Eq. 2}$$

Where, w_a, w_b and w_i (gm) are the weights of samples after and before deposition, and the total injected powder, respectively. The w_i is calculated as;

$$w_i = F * l / V \quad \text{Eq. 3}$$

Where, F is the powder feed rate ($gm.s^{-1}$), l is the clad track length (mm) and V is the scan speed ($mm.s^{-1}$). The powder efficiency of Aluminum and its composites increases with increasing the E, while a slightly increasing of powder efficiency is noticed as changing from SiC to Mo, Figure 7. Previous studies have reported that the low E is unable to melt the entire powder resulting in reduced powder efficiency. With increasing E, more powder melts and reduces powder loss, thus increasing the powder efficiency(4,19,22). While using Al-SiC clad with heat input above 22.93 $J.mm^{-2}$ we can observe unexpected phenomena that catchment efficiency decreased due to detachment of full layer from the substrate **Fig. 1**. This can be explained that at high temperature, Aluminum tend to reject SiC particles at the top and agglomerate which lead to a SiC layer that didn't diffuse with Aluminum.

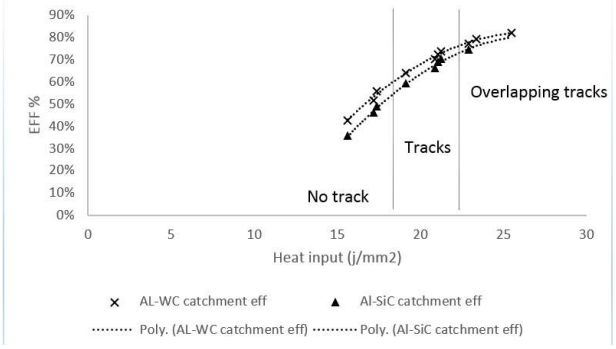

Fig. 1 variation of Powder Efficiency, η with Laser Energy density E

The morphology of clad tracks, when using Aluminum powder and its composite of 30% SiC and 30% Mo on mild steel substrate at different laser energy density **(**E), is shown in Figure 3 and Figure 4, respectively. The figures describe gradually formation of clad layer, from separate particles at E of 15.63 $J.mm^{-2}$ to full **-**clad layer at E of 22.93 $J.mm^{-2}$. First; tracks are formed in a gradual manner at laser energy density from E of 15.63 $J.mm^{-2}$ to 19.11 $J.mm^{-2}$, beyond which the width of tracks increases gradually with increasing E thus overlapping until the whole substrate surface is covered with uniform layer with wavy surface at E = 22.93 $J.mm^{2}$.

3.2 Single Track Formation

Multiple single tracks are formed gradually as shown in Figure 3 and figure 4 (a – d) for the clad powders Aluminum and its composites 30% SiC and 30% Mo, respectively. Generally, patterns formation with changing E is similar in both cases. This can be described as: 1) Weak and small powder agglomerates stacked on substrate at laser energy density 15.64 J.mm-2, **Fig. 2**-a and **Fig. 3**-a, 2) Semi track agglomerates formation at laser energy density of 17.37 J.mm-2, **Fig. 2**-b **Fig. 3**-b, Enlargement of this semi tracks to form continuous track , at 21.23 J.mm^{-2} **Fig. 2**-c and **Fig. 3**-c. 4) Track overlapping and layer formation , at E of 22.93 J.mm-2, **Fig. 2**-e and **Fig. 3**-e. At the same E, patterns formation is generally bigger in case of Mo powder composite with 30% Mo compared to 30% SiC powder. As reported in previous work, this can be attributed to the differences in absorption of laser energy between Mo and SiCp [31].

It can be also seen in **Fig. 2**, that the surface morphology becomes darker while using SiCp into the clad powder. Similar observation is reported by previous researchers, which has analyzed to burning of free carbon which formed after dissolution of SiCp (17). The dark color of deposited tracks can be removed by cleaning methods (17).

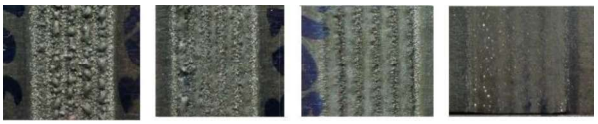

a. 15.63 (J/mm^2) b. 17.37 (J/mm^2) c. 21.23 (J/mm^2) d. 22.93 (J/mm^2)

Fig. 2 Macro photographs of clad surfaces for Aluminum composite of 30 wt.% SiCp produced at different E

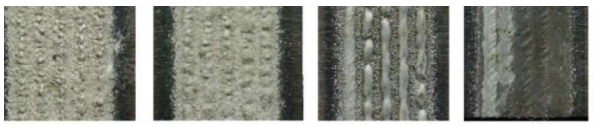

b.15.63 (J/mm^2)	b. 17.37 (J/mm^2)	c. 21.23 (J/mm^2)	d. 22.93 (J/mm^2)

Fig. 3 Macro photographs of clad surfaces for Aluminum composite of 30 wt.% Mo produced at different E

From present and previous work (4,17), the gradual formation of single tracks with increasing E can be schematically presented as in **Fig. 4**. It can be observed that the gradual formation of tracks passes through two main stages; interrupted tracks (no cladding and detached tracks) and multiple single tracks, **Fig. 4** a - f. No-cladding occurred and weakly particles are stacked on the substrate surface, **Fig. 4** - a, b. Detached tracks appeared and formed from globular melted metal due to increasing the laser energy density (increasing the laser power or decreasing the scan speed), **Fig. 4**- c. The shapes of detached tracks changed from spherical to slightly elongated shapes in **Fig. 4** c, d and e. With higher E, the detached tracks were connected and formed continuous and uniform thin single tracks **Fig. 4** - f.

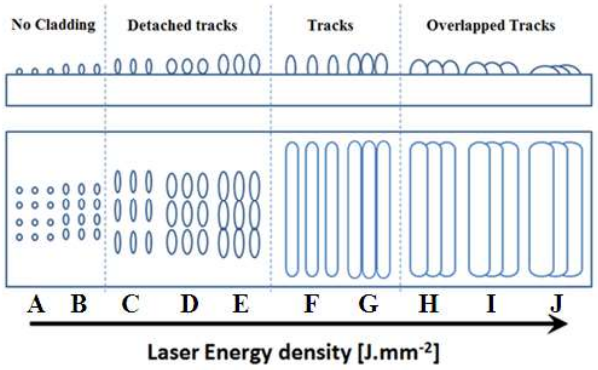

Fig. 4 Schematic representation of tracks formation

3.2 Single Track geometry

Final clad layer profile formed by overlapped tracks, depends on the shape and geometry of cladding tracks (4,19).The regular shape of a continuous formed single track is presented, for example, by the photomicrograph in **Fig. 5**, for Aluminum composite 30% Mo powder, produced at E of 19.11 J.mm^{-2}. A schematic presentation describes the track geometry in the transverse direction by track width (W), track height (H) and track depth of penetration (B), **Fig. 6**.

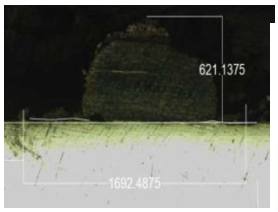

Fig. 5 Track cross section of Aluminum composite 30 wt.% Mo produced at E =19.11 J.mm^{-2}

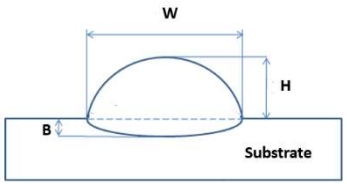

Fig. 6 Schematic representation of track geometry

The evolution of track geometrical dimensions and features with various laser energy density E, for Aluminum composites of 30% SiCp and 30% Mo, is represented in **Fig. 7-11**. The figure also includes previous results of stainless steel with SiC on steel (23).

Track width is directly proportional with the laser energy density, **Fig. 7**. This observations has been discussed in earlier investigations as due to the increase in the temperature of the melt pool, which led to the increase in

the rate of powder catchment (19,20,22). By lowering laser scan speed, longer interaction time results which leads to increasing deposition thus increasing track width.

Track height is inversely proportional with the laser energy density, while the penetration is directly proportional, **Fig. 8** .As discussed in previous researches (19,22), this phenomena can be explained by the rise in molten pool of the aluminum and steel substrate surface temperatures, leads to the increase of track penetration on account of height reduction (19,20,22).

In previous researches (4,19–22), more features are calculated; namely aspect ratio (A_R), which is the ratio between track width and track height, and dilution percentage (D) which is the ratio of interference between substrate and clad layer, those features are calculated as follow:

$$\mathbf{A_R} = W / H \qquad \text{Eq. 4}$$

$$\mathbf{D} = (B / (H + B)) * 100 \qquad \text{Eq. 5}$$

Fig. 7-11 shows changes associated with the increase of laser energy density of different track geometry aspects. The increase in track width W **Fig. 7** , penetration depth **Fig. 9** and decrease in track height H **Fig. 8** is reflected on increasing aspect ratio A_R **Fig. 10** and Dilution Percentage D **Fig. 11** as calculated by equation 3.

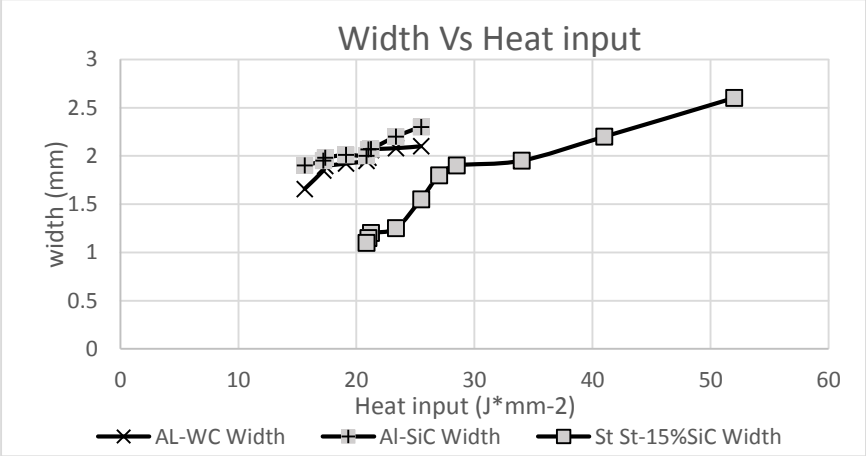

Fig. 7 the effect of laser energy density on clad layer width for Aluminum and its composites of 30% SiC and 30% Mo with previous work stainless steel 431 and 15%SiC(23)

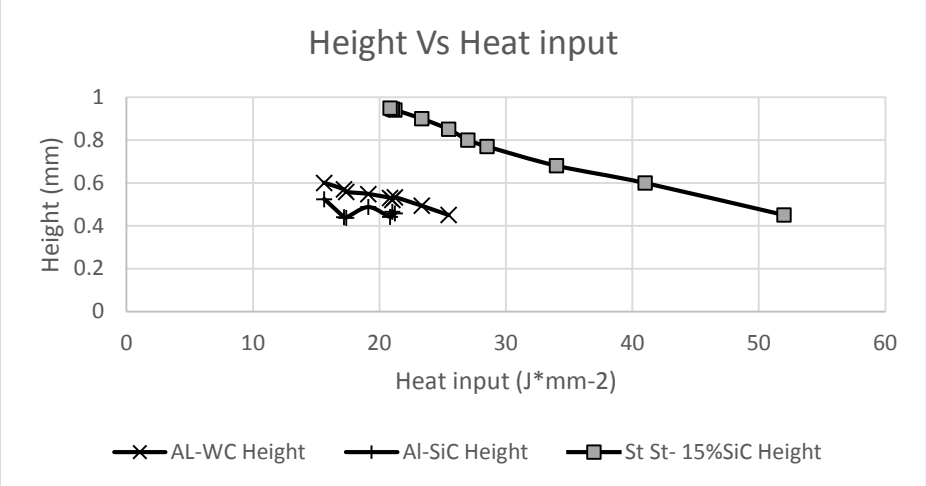

Fig. 8 the effect of laser energy density on clad layer height for Aluminum and its composites of 30% SiC and 30% Mo with previous work stainless steel 431 and 15%SiC(23)

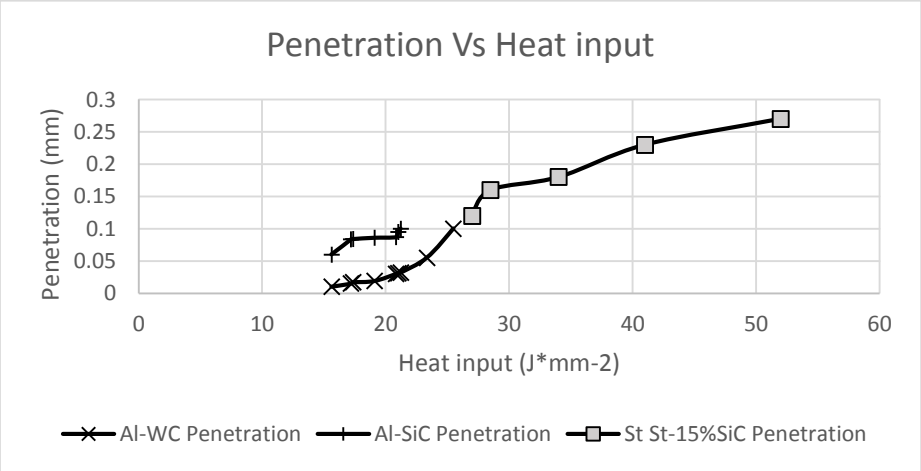

Fig. 9 the effect of laser energy density on clad layer penetration for Aluminum composites of 30% SiC and 30% Mo with previous work stainless steel 431 and 15%SiC(23)

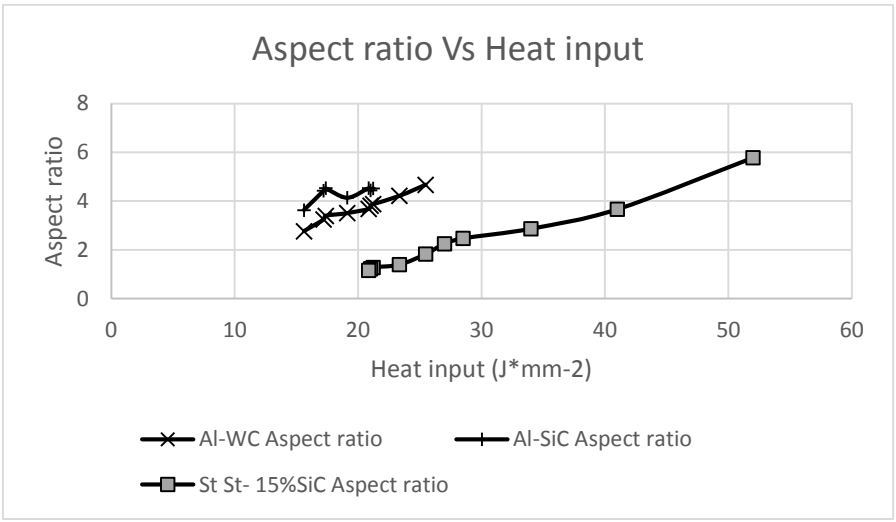

Fig. 10 the effect of laser energy density on clad layer Aspect ratio for Aluminum composites of 30% SiC and 30% Mo with previous work stainless steel 431 and 15%SiC(23)

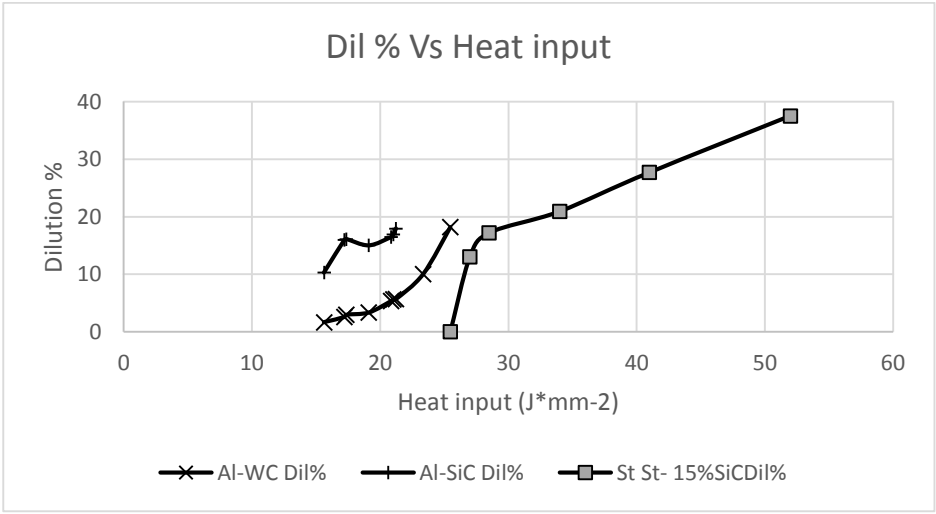

Fig. 11 the effect of laser energy density on clad layer Dilution % for Aluminum composites of 30% SiC and 30% Mo with previous work stainless steel 431 and 15%SiC(23)

From the above results we can observe that the clad width change relative to changing material of clad composite, this observation leads us to go further in the reasons of the increase of the clad width due to change in clad material. Previous research reported that the clad material spread is dependent on clad material absorptivity (24),clad material melting temperature, clad material flow ability and clad – substrate materials chemical interface (25).

In this investigation we have changed the ceramic component in the clad material once from Al-SiC to Al-Mo and compared the change of the host material of the ceramic from Al-SiC to St.St-SiC with previous research paper (23). From the mentioned matrix we can investigate the effect of changing the ceramic material in the clad and the change of the host material.

The reported increase in width with the change in the host material from Stainless steel – 15% silicon carbide to Aluminum 30% silicon - carbide can be explained by decrease of metal melting temperature from stainless steel with melting temperature of 1400-1450 C to pure Aluminum melting temperature of 660 C. Also the increase in SiC content lead to increase the absorptivity as reported previously (26). Another aspect affect the width increase due to change from Stainless steel to Aluminum is

4. Conclusions

Cladding layer formation steps in laser cladding of pure Aluminum and its composites of 30 wt. % SiC and 30% wt. % Mo, are: Detached tracks, single tracks and overlapped tracks. The cladding layer formation and geometry are direct result to the change of laser energy density. The single track geometry (width, depth of penetration, aspect ratio and dilution) increases with the increase of the laser energy density, while the height is decrease. The influence of SiCp addition rather than Mo is such that as we use SiCp, the tracks width, height, penetration and dilution percentage increase, while the aspect ratio decreases. For accepted quality, the recommended processing parameters throughout the implemented experiments, for deposition of pure Aluminum and its composites layer are 1200 w laser power and 1 $m.min^{-1}$ scan speed, which equal to 22.93 $J.mm^{-2}$ laser energy density.

References:

[1]. 1. Chew Y, Pang JHL. Fatigue life prediction model for laser clad AISI 4340 specimens with multiple surface cracks. Int J Fatigue. 2016;87:235–44.

[2]. 2. Cottam R, Brandt M. Laser cladding of Ti-6Al-4V powder on Ti-6Al-4V substrate: Effect of laser cladding parameters on microstructure. Phys Procedia. 2011;12(PART 1):323–9.

[3]. 3. Huang J, Li Z, Cui H, Yao C, Wu Y. Laser welding and laser cladding of high performance materials. Phys Procedia [Internet]. 2010;5(PART 2):1–8. Available from: http://dx.doi.org/10.1016/j.phpro.2010.08.023

[4]. 4. Ocelík V, Nenadl O, Palavra A, De Hosson JTM. On the geometry of coating layers formed by overlap. Surf Coatings Technol [Internet]. 2014;242:54–61. Available from: http://dx.doi.org/10.1016/j.surfcoat.2014.01.018

[5]. 5. Lee HK. Effects of the cladding parameters on the deposition efficiency in pulsed Nd:YAG laser cladding. J Mater Process Technol. 2008;202(1–3):321–7.

[6]. 6. Zeng C, Tian W, Liao WH, Hua L. Microstructure and porosity evaluation in laser-cladding deposited Ni-based coatings. Surf Coatings Technol. 2016;294:122–30.

[7]. 7. Choi J, Chang Y. Characteristics of laser aided direct metal/material deposition process for tool steel. Int J Mach Tools Manuf. 2005;45(4–5):597–607.

[8]. 8. Zhou C, Zhao S, Wang Y, Liu F, Gao W, Lin X. Mitigation of pores generation at overlapping zone during laser cladding. J Mater Process Technol [Internet]. 2015;216(1):369–74. Available from: http://dx.doi.org/10.1016/j.jmatprotec.2014.09.025

[9]. 9. Pei YT, Ocelik V, De Hosson JTM. SiCp/Ti6Al4V functionally graded materials produced by laser melt injection. Acta Mater. 2002;50(8):2035–51.

[10]. 10. Smurov I. Laser cladding and laser assisted direct manufacturing. Surf Coatings Technol. 2008;202(18):4496–502.

[11]. 11. Association A. Aluminum: properties and physical metallurgy. ASM international; 1984.

[12]. 12. El-Kady O, Fathy A. Effect of SiC particle size on the physical and mechanical properties of extruded Al matrix nanocomposites. Mater Des [Internet]. 2014;54(December):348–53. Available from: http://dx.doi.org/10.1016/j.matdes.2013.08.049

[13]. 13. Dutta Majumdar J, Kumar A, Li L. Direct laser cladding of SiC dispersed AISI 316L stainless steel. Tribol Int. 2008;42(5):750–3.

[14]. 14. Majumdar JD, Li L. Studies on direct laser cladding of SiC dispersed AISI 316L stainless steel. Metall Mater Trans A Phys Metall Mater Sci. 2009;40(12):3001–8.

[15]. 15. Abbas G, Ghazanfar U. Two-body abrasive wear studies of laser produced stainless steel and stainless steel + SiC composite clads. Wear. 2005;258(1-4 SPEC. ISS.):258–64.

[16]. 16. Tassin C, Laroudie F, Pons M, Lelait L. Improvement of the wear resistance of 316L stainless steel by laser surface alloying. Surf Coatings Technol. 1996;80(1–2):207–10.

[17]. 17. Brytan Z, Dobrzański L a, Pakieła W. Laser

surface alloying of sintered stainless steels with SiC powder. J Achiev Mater Manuf Eng. 2011;47(1):42–56.

[18]. 18. Van Acker K, Vanhoyweghen D, Persoons R, Vangrunderbeek J. Influence of tungsten carbide particle size and distribution on the wear resistance of laser clad WC/Ni coatings. In: Wear. 2005. p. 194–202.

[19]. 19. Ya W, Pathiraj B, Liu S. 2D modelling of clad geometry and resulting thermal cycles during laser cladding. J Mater Process Technol. 2016;230:217–32.

[20]. 20. Noskov AI, Gilmutdinov AK, Yanbaev RM. Effect of coaxial laser cladding parameters on bead formation. Int J Miner Metall Mater. 2017;24(5):550–6.

[21]. 21. de Oliveira U, Ocelík V, De Hosson JTM. Analysis of coaxial laser cladding processing conditions. Surf Coatings Technol. 2005;197(2–3):127–36.

[22]. 22. Hemmati I, Ocelík V, De Hosson JTM. The effect of cladding speed on phase constitution and properties of AISI 431 stainless steel laser deposited coatings. Surf Coatings Technol [Internet]. 2011;205(21–22):5235–9. Available from: http://dx.doi.org/10.1016/j.surfcoat.2011.05.035

[23]. 23. Taha MA. Direct laser cladding of stainless steel powder and its composite with SiC.

[24]. 24. Sabuj SR, Hamamura M. Random cognitive radio network performance in Rayleigh-lognormal environment. 2017 14th IEEE Annu Consum Commun Netw Conf CCNC 2017. 2017;6(3):992–7.

[25]. 25. Nurminen J, Näkki J, Vuoristo P. Microstructure and properties of hard and wear resistant MMC coatings deposited by laser cladding. Int J Refract Met Hard Mater [Internet]. 2009;27(2):472–8. Available from: http://dx.doi.org/10.1016/j.ijrmhm.2008.10.008

[26]. 26. Amir rahimpour Shayan. Laser absorption for Si & SiC. West Michigan Univ. 2008;

[27]. 27. Prashanth KG, Scudino S, Maity T, Das J, Eckert J. Is the energy density a reliable parameter for materials synthesis by selective laser melting? Mater Res Lett [Internet]. 2017;5(6):386–90. Available from: http://dx.doi.org/10.1080/21663831.2017.1299808

[28]. 28. Ocelík V, Nenadl O, Hemmati I, Hosson JTM De. Thickness and waviness of surface coatings formed by overlap : modelling and experiment. 78:135–44.